INTERACTION OF VORTEX BREAKDOWN WITH A FLEXIBLE FIN AND ITS CONTROL, PHASE-2.

Final Report

submitted to

Dr. Charbel N Raffoul
Chief of Aeronautical Sciences
European Office of Aerospace Research & Development (EOARD)
223/231 Old Marylebone Road
NW1 5TH London, UK

by

Dr. Ismet Gursul
Department of Mechanical Engineering
University of Bath
Bath, BA2 7AY
United Kingdom

February 13, 2001

AQ FO1-06-0975

REPORT DOCUMENTATION PAGE

Form Approved OMB No. 0704-0188

Public reporting burden for this collection of information is estimated to average 1 hour per response, including the time for reviewing instructions, searching existing data sources, gathering and maintaining the data needed, and completing and reviewing the collection of information. Send comments regarding this burden estimate or any other aspect of this collection of information, including suggestions for reducing this burden to Washington Headquarters Services, Directorate for Information Operations and Reports, 1215 Jefferson Davis Highway, Suite 1204, Arlington, VA 22202-4302, and to the Office of Management and Budget, Paperwork Reduction Project (0704-0188), Washington, DC 20503.

1. AGENCY USE ONLY (Leave blank)	2. REPORT DATE	3. REPORT TYPE AND DATES COVERED
	13-February-2001	Final Report

4. TITLE AND SUBTITLE

Interaction of Vortex Breakdown with a Flexible Fin and its Control, Phase-2

5. FUNDING NUMBERS

F61775-00-WE025

6. AUTHOR(S)

Dr. Ismet Gursul

7. PERFORMING ORGANIZATION NAME(S) AND ADDRESS(ES)

University of Bath
Claverton Down
Bath BA2 7AY
United Kingdom

8. PERFORMING ORGANIZATION REPORT NUMBER

N/A

9. SPONSORING/MONITORING AGENCY NAME(S) AND ADDRESS(ES)

EOARD
PSC 802 BOX 14
FPO 09499-0200

10. SPONSORING/MONITORING AGENCY REPORT NUMBER

SPC 00-4025

11. SUPPLEMENTARY NOTES

12a. DISTRIBUTION/AVAILABILITY STATEMENT

Approved for public release; distribution is unlimited.

12b. DISTRIBUTION CODE

A

13. ABSTRACT (Maximum 200 words)

This report results from a contract tasking University of Bath as follows: The contractor will investigate the fin buffeting caused by vortex breakdown and its control. In this phase, a flexible fin will be designed and fabricated. It consists of a thin brass spar surrounded by several balsa wood segments to provide aerodynamic shaping. Fin vibration levels will be sensed by root strain gages and tip accelerometers. Unsteady surface pressure measurements on the delta wing and underneath the vortex will be carried out in order to detect and quantify the oscillations of vortex breakdown location due to fin vibrations. Also, flow velocity measurements and visualization experiments will be carried out in U. of Bath water tunnel.

14. SUBJECT TERMS

EOARD, Aero-Structure Interface, Aeroelasticity, Fin Buffeting

15. NUMBER OF PAGES

24

16. PRICE CODE

N/A

17. SECURITY CLASSIFICATION OF REPORT	18. SECURITY CLASSIFICATION OF THIS PAGE	19, SECURITY CLASSIFICATION OF ABSTRACT	20. LIMITATION OF ABSTRACT
UNCLASSIFIED	UNCLASSIFIED	UNCLASSIFIED	UL

NSN 7540-01-280-5500

Standard Form 298 (Rev. 2-89)
Prescribed by ANSI Std. 239-18
298-102

Abstract

Buffeting of a flexible fin due to the leading-edge vortex flow over a delta wing was investigated. Tip acceleration of the fin as well as unsteady wing and fin surface pressure were measured to understand the interaction of the fin with vortex breakdown. It was found that structural resonances occur only at high angle of attack range ($\alpha=30°$-$40°$), whereas the dimensionless acceleration is roughly constant at lower angles of attack. Maximum buffeting response occurs when the fin is located near the vortex axis for low angles of attack, but the location of the maximum buffeting shifts to inboard locations as the angle of attack is increased. The results show that single-fin buffeting may be more important than twin-fin buffeting. Simultaneous measurements of the fin acceleration and the wing surface pressure underneath the leading-edge vortex provide evidence on the extent of vortex-fin interactions. Even in the absence of vortex breakdown, effect of fin vibrations is observed far upstream of the fin.

1. Introduction

A typical fighter aircraft performs maneuvers at high angle of attack. Separated vortical flows originating from delta wings, leading-edge extensions, and forebodies interact with wings, fins and tails. Vortex breakdown phenomenon is the most important source of buffeting over delta wings, the most famous example of this is the F/A-18 fin buffeting. The vertical tails are in the highly unsteady flow of vortex breakdown wake as shown in Figure 1 causing large structural vibrations and severe structural fatigue damage. A summary of previous investigations is given by Wolfe et al (1995) and Gursul and Xie (1999).

The interaction of vortex breakdown with a fin is a complicated process affected by: time-averaged breakdown location, helical mode instability of the flow downstream of breakdown, quasi-periodic oscillations of breakdown location, unsteady flow separation from the leading-edge of the fin, possible coupling between the flow separation and vortex breakdown with a feedback effect, and aeroelastic deflections of the fin. In addition, aeroelastic deflections of the fin may provide a feedback effect on vortex breakdown and disturbances due to aeroelastic effects (surface deflections) may propagate upstream, resulting in large oscillations of breakdown location. The feedback effect of fin oscillations was not considered in detail previously, although the

2

sensitive nature of vortex breakdown to small changes, and the subcritical nature of the flow (for which the disturbances may propagate upstream) are well known.

Gursul and Xie (2000) experimentally simulated aeroelastic deflections of a fin in the first bending mode by the forced oscillations of a rigid fin about a hinge, because this mode of buffeting is the most dangerous. Flow visualization showed that the fin deflections may be important depending on the fin location with respect to the leading-edge vortex (see Figure 2). Vortex breakdown location is not sensitive to the static deflections of the fin when it is well upstream of the fin, for example for $y_f/s=0.6$. However, when the breakdown location is near, or downstream, of the fin (for example, for $y_f/s=0.3$) it is very sensitive to the static deflections of the fin. Hence this type of configuration may cause coupling of vortex breakdown and fin oscillations.

This approach chosen by Gursul and Xie (2000) eliminates structural resonance which occurs when the excitation frequency of the vortex flow coincides with the natural frequency of the fin. The amplitude of the fin oscillations was kept fixed while the frequency was varied. Results show that the response of breakdown location to an oscillating fin is similar to that of a lowpass filter. For frequencies higher than a cutoff frequency, vortex breakdown does not respond to fin oscillations. A mechanism based on the subcritical flow and wave propagation characteristics of the vortex flows was proposed to explain these observations.

In this investigation the main objective is to develop a more complex and realistic model by using a flexible fin. The main parameter is the natural frequency of the fin, while the amplitude of the vibration is determined by the unsteady vortex flow, which may have multiple excitation frequencies. The feedback effect of fin vibrations on vortex breakdown and possible nonlinear interaction of the fin with vortex breakdown are investigated by measurements of fin-buffeting response, unsteady wing and fin surface pressure, and flow visualization.

2. Experimental Setup

A flexible fin shown in Figure 3a was designed and fabricated. It consists of a thin aluminum spar surrounded by several wood segments to provide aerodynamic shaping. The advantages that the wood sections offer are low material density and ease of fabrication. These sections were attached to the spar with small bolts. With this design, the contribution of the airfoil sections to the bending stiffness of the spar is

3

minimized. The dimensions of the spar were chosen to obtain the natural frequencies of the first bending mode for a typical modern combat aircraft. The thickness of the spar was 2 mm. The leading-edge of the fin was double bevelled at an angle of 30 deg. The main dimensions of the fin are given in Figure 3a. The spar was attached to the delta wing by a bracket near the trailing-edge of the wing.

Experiments were carried out for this configuration in a 2.12 m by 1.51 m low-speed wind tunnel. The experimental setup, which uses a half-model delta wing and a splitter plate, is shown in Figure 3b. The delta wing model had a sweep angle of $\Lambda=75°$ and a chord length of c=500 mm. The lee surface was flat, whereas the leading-edges were bevelled at 45° on the windward side. The thickness of the delta wing was 15 mm. The Reynolds number based on the chord length varied from Re=$3.5*10^5$ to $1*10^6$. The dimensions of the delta wing and fin are scaled to those used in the water tunnel experiments by Gursul and Xie (2000).

As a first step, buffeting response of this flexible fin was investigated. Fin vibration levels were sensed by a tip accelerometer. In addition to the calculating the rms value of the fin tip acceleration, the spectra of the tip acceleration was examined for each case. The lowest dominant frequency of the fin vibrations is shown in Figure 4 as a function of free stream velocity. It is seen the frequency, which is the natural frequency of the first bending mode, is nearly constant. In addition, there is little influence of the angle of attack on the vibration frequency.

Flow visualization was performed using an Aerotech paraffin smoke generator. The wind tunnel was run at 3 m/s (this speed was decided upon in order to maintain a Reynolds number of approximately 100,000). A Panasonic digital video camera was used to capture flow visualization images. At selected spanwise positions of the fin (y_f/s=0.2, 0.4, 0.6, 0.8, and 1.0), images were taken from the side of the tunnel and from underneath the wind tunnel for side and top views of the leading-edge vortex.

Unsteady surface pressure measurements were made by miniature pressure transducers (Entran), which are suitable for low-pressure measurements with high sensitivity (150 mV/psi). The pressure transducers were installed within the model delta wing and the fin due to their small size, and were used for simultaneous measurement of pressure fluctuations on the wing surface and fin together with the tip acceleration. The flush mounted transducers eliminated the need for calibration and correction for the amplitude attenuation and phase distortion due to transmission lines,

4

while the size of pressure sensing area (less than 2 mm^2) was still acceptable. One of the pressure transducers was located on the wing surface and underneath the vortex. The spanwise location of the vortex was estimated from the pressure measurements across the span at x/c=0.5 in the absence of the fin. It is seen in Figure 5 that the location of the pressure (suction) peak is only slightly affected by the angle of attack, showing that the spanwise location of the leading edge vortex is roughly constant. Consequently, it was decided to place the transducer at y/s=0.6. The measurement uncertainty for the surface pressure was estimated as 4%.

3. Results

As mentioned earlier, the main variables are the natural frequencies of the fin, the vortex excitation frequency f_e (hence free stream velocity U_∞, since $f_e c/U_\infty$ is roughly constant), and vortex-fin configuration characterized by angle of attack α and normalized fin location y_f/s. The tip acceleration was being measured as a function of these variables. The variation of root-mean-square value of acceleration as a function of free stream velocity for different values of angle of attack is shown in Figure 6 for y_f/s=0.2 to 1.0 with increments of 0.1. As expected, for a given configuration, the rms acceleration increases with increasing free stream velocity. Local maximums are observed around certain U_∞ (particularly at low speeds) and at high angle of attack due to the structural resonances. Tip acceleration increases with U_∞ away from resonance conditions.

A more appropriate form of presenting the data is the variation of dimensionless acceleration parameter, which includes the effect of the free stream velocity. If the rms acceleration a_{rms}, free stream velocity U_∞, and the spar thickness t are considered as main variables, a dimensionless number $a_{rms} t / U_\infty^2$ can be formed. A similar approach was used by Mabey (1973) in presenting the tip acceleration data. The variation of dimensionless acceleration as a function of free stream velocity (corresponding to the data shown in Figure 6), is shown in Figure 7. It can be seen that the dimensionless acceleration is constant for low and moderate angles of attack over the free stream velocity range tested, but for higher angles of attack, there is a local maximum near the low speed end. This indicates a possible resonance with the helical mode instability of

vortex breakdown. For example, for $y_f/s=0.4$ and $\alpha=40°$, the local maximum occurs at $U_\infty=12$ m/s, which corresponds to a dimensionless frequency of $fc/U_\infty=1.37$ (where the f is the frequency of the fin vibrations). This value compares reasonably well with the measurements of the helical mode instability over delta wings, which revealed that fc/U_∞ is around 1.20 at $\alpha=40°$ (Gursul, 1994). For $U_\infty \geq 15$ m/s, the dimensionless acceleration is approximately constant even at higher angles of attack. For low angles of attack ($\alpha=10°$-$20°$), the structural resonance is absent, which is presumably related to the excitation characteristics in the vortex flow.

The data presented here indicate very strong effects of the fin location and angle of attack. The variation of the rms tip acceleration with the fin location is shown in Figure 8 for $U_\infty=30$ m/s. It is seen that the buffeting response is very small for the most outboard fin location ($y_f/s=1.0$) for all angles of attack. The maximum buffeting response occurs near the vortex axis ($y_v/s\approx0.60$) for low angles of attack, although this is a very broad peak. As the angle of attack is increased, the local maximum with very well defined peaks shifts to inboard locations. However, note that the spanwise location of the vortex axis does not change much with angle of attack (see Figure 5). Hence, the shift in the location of the maximum buffeting response is likely due to the direct impingement of the shear layer in the breakdown region onto the fin.

In order to understand this interaction better, flow visualization was performed. Figure 9 shows flow visualization pictures as a function of fin location y_f/s for $\alpha=30°$. Note that $y_f/s=0.4$ produces the largest buffeting response. It is interesting that inboard fin locations cause larger buffeting response than outboard locations. The physical mechanism behind this asymmetric response is not clear. Variation of breakdown location as a function of fin location at different angles of attack is shown in Figure 10. Comparison of this figure with the tip acceleration shown in Figure 8 amplify the importance of fin postion even when breakdown location is nearly the same for large angle of attack.

Note that largest buffeting response occurs for the most inboard fin locations ($y_f/s=0.2$ and 0.3) at the highest angles of attack ($\alpha=35°$-$40°$). Hence there is an apparent asymmetry with regard to the effect of fin location on the buffeting response. This result also implies that single-fin buffeting may be as important as twin-fin buffeting. The location of vortex breakdown and the relative position of the shear layer

with respect to the fin, as well as the variation of the strength of the vortices as the angle of attack varies are likely be important factors.

Figure 11 shows the variation of the rms tip acceleration as a function of angle of attack for different fin locations. Maximum buffeting response occurs for $\alpha=30°$-$40°$ depending on the fin location. The most dramatic variations occur for $y_f/s=0.2$. For this fin location, there is very little buffeting at low to moderate angles of attack (up to $\alpha=30°$), but there is a very sharp increase in buffeting at $\alpha=35°$ and $40°$. Corresponding flow visualization pictures are shown in Figure 12. The picture for $\alpha=35°$ indicates that the shear layer of the breakdown region impinges onto the fin. For other fin locations shown in Figure 11, the variation of buffeting response with angle of attack is more gradual. An interesting case is for $y_f/s=0.6$ for which vortex breakdown is always upstream of the fin. In this case, the fin buffeting response first increases with angle of attack, and then remains nearly constant at high angle of attack. For fin locations $y_f/s=0.8$ and 1.0, it is seen that the buffeting response actually decreases at high angle of attack.

As mentioned earlier, simultaneous measurements of pressure fluctuations on the wing surface underneath the vortex ($y/s=0.6$) and the fin tip acceleration were conducted for the fin position $y_f/s=0.4$. The location of the pressure transducer was varied in the streamwise direction in order to understand the extent of the vortex-fin interaction. The variation of the coherence function between the wing pressure and fin acceleration is shown in Figure 13 for varying streamwise locations of the pressure transducer and at different angles of attack. It is seen that at low angles of attack there is a peak corresponding to the fin natural frequency in the first bending mode. It is remarkable that this peak is observed at upstream locations as far as $x/c=0.15$. This shows the upstream influence of the fin vibrations on the vortex flow. However, since there is no vortex breakdown at low angles of attack, the vortex flow is supposed to be supercritical and waves cannot propagate upstream in supercritical flows. Therefore wave propagation characteristics of vortex cores cannot explain the experimental results presented in Figure 13. It is interesting that as the angle of attack increases, the coherence between the two signals is lost for upstream locations (see $x/c=0.15$, 0.39, and 0.62). The observed coherence at low angles of attack when the vortex is compact (i.e., without breakdown) may be due to the oscillations of the vortex core as a result of the oscillations of the fin. It cab also be seen that, for streamwise locations near the fin

7

(x/c=0.86 and 0.98), there are broad peaks of coherence at higher frequencies at high angles of attack. This is not clearly understood and further analysis is underway.

4. Conclusions

In this investigation, buffeting of a flexible fin due to the leading-edge vortex flow over a delta wing was investigated. Tip acceleration of the fin as well as unsteady wing and fin surface pressure were measured to understand the interaction of the fin with vortex breakdown. Fin-buffeting response strongly depends on the free stream velocity, and vortex-fin configuration which is characterized by angle of attack and fin location. A dimensionless acceleration parameter was found to be more appropriate to present the buffeting response. It was found that structural resonances occur only at high angle of attack range ($\alpha=30°-40°$) whereas the dimensionless acceleration is roughly constant at lower angles of attack. Maximum buffeting response occurs when the fin is located near the vortex axis for low angles of attack, but the location of the maximum buffeting shifts to inboard locations as the angle of attack is increased. The results show that single-fin buffeting may be more important than twin-fin buffeting. Simultaneous measurements of the fin acceleration and the wing surface pressure underneath the leading-edge vortex, and subsequent analysis of cross-correlation provide evidence on the extent of vortex-fin interactions. At low angles of attack where there is no vortex breakdown, substantial correlation between the surface pressure and fin acceleration was found. Effect of fin vibrations is observed at upstream locations as far as x/c=0.15, although the physical mechanism of this upstream influence is less clear.

Acknowledgment

References

Gursul, I., 1994, "Unsteady Flow Phenomena over Delta Wings at High Angle of Attack", *AIAA Journal*, vol. 32, no. 2, 1994, pp.225-231.

Gursul, I., and Xie, W., 1999, "Buffeting Flows over Delta Wings", *AIAA Journal,* vol. 37, no. 1, pp. 58-65.

Gursul, I. and Xie, W., 2000, "Interaction of Vortex Breakdown with an Oscillating Fin", accepted for publication in *AIAA Journal*, see also AIAA-2000-0279, 38th Aerospace Sciences Meeting and Exhibit, January 10-13, Reno, NV.

Mabey, D.G., "Beyond the Buffet Boundary", *Aeronautical Journal,* vol. 77, April 1973, pp. 201-215.

Wolfe, S., Canbazoglu, S., Lin, J.C. and Rockwell, D., "Buffeting of Fins: An Assessment of Surface Pressure Loading", *AIAA Journal,* vol. 33, no. 11, 1995, pp. 223-2234.
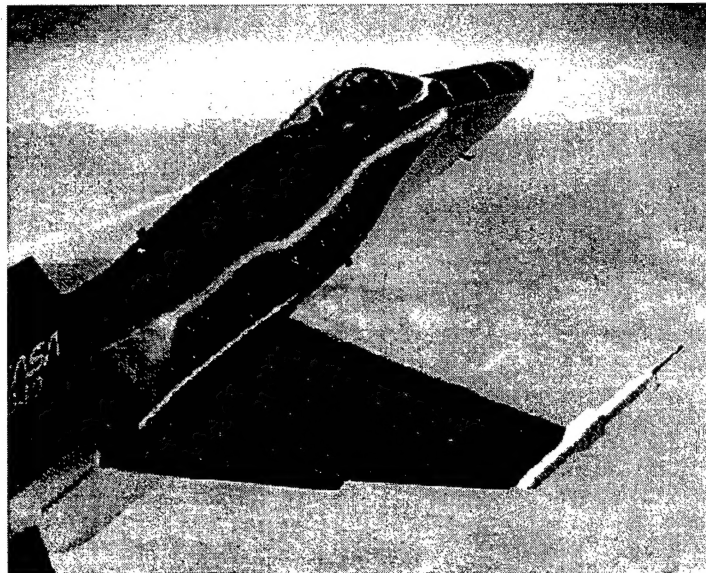
Figure 1: NASA flow visualization picture of vortex breakdown over F/A-18.
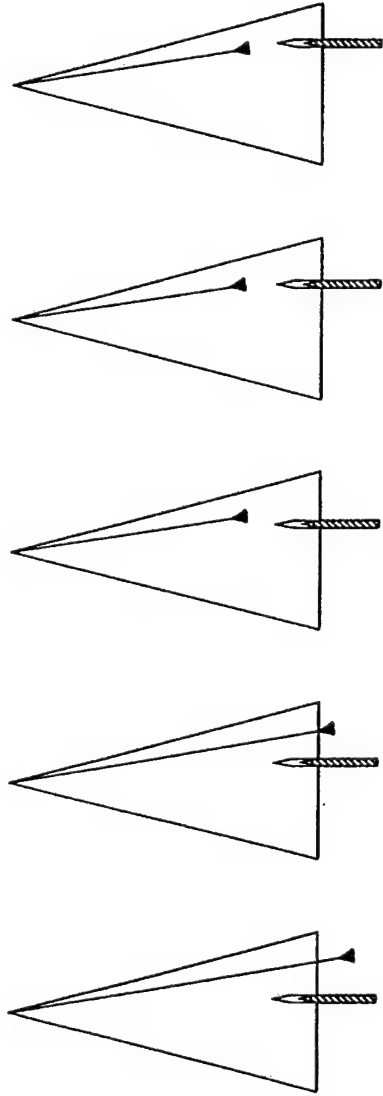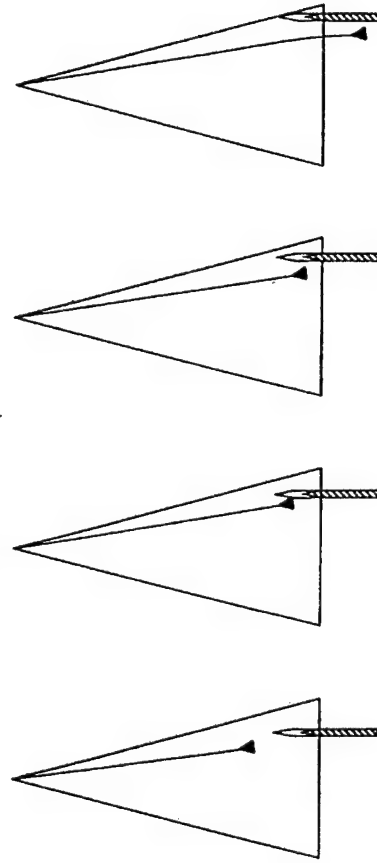
igure 2: Time-averaged breakdown location for no fin deflection, $\alpha = 20^0$
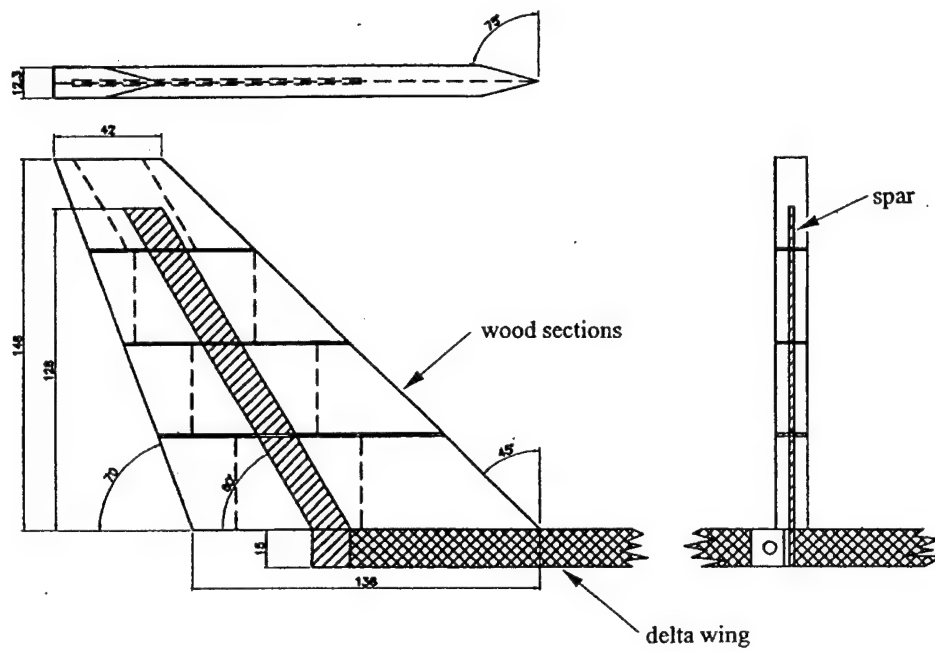
(a) Design of flexible fin.
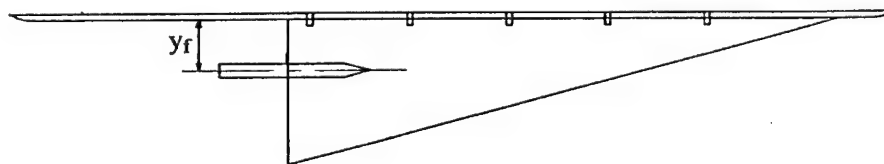
(b) Half- delta wing model, fin, and splitter plate.

Figure 3: Overview of the experimental setup.
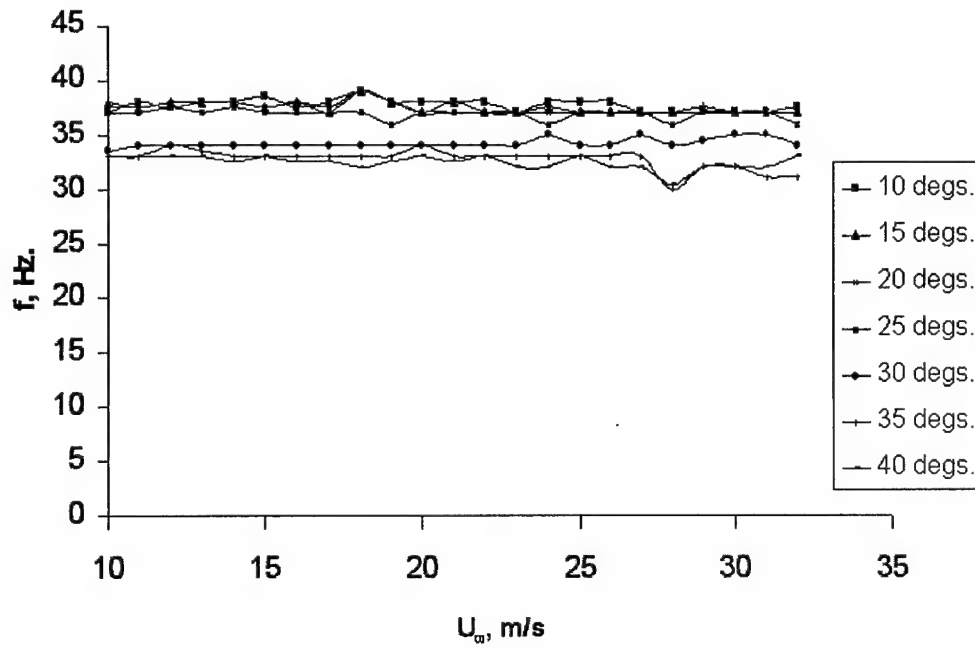
Figure 4: Variation of natural frequency of first bending mode as a function of free stream velocity, $Y_f/s = 0.4$.
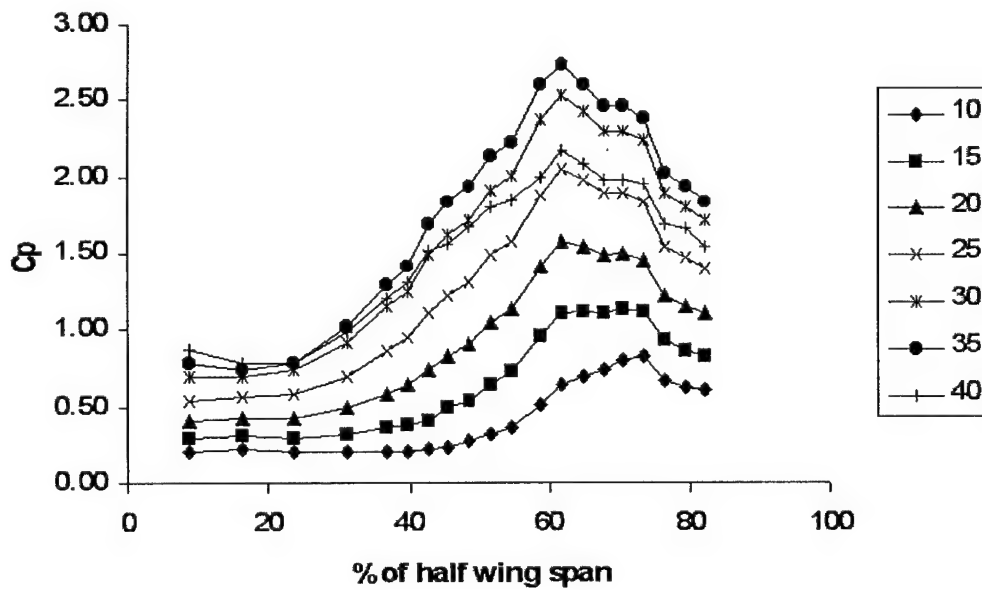
Figure 5: Variation of pressure coefficient as a function of spanwise distance, x/c = 0.5
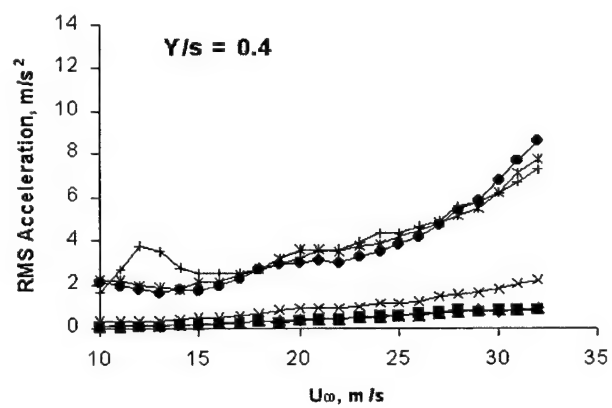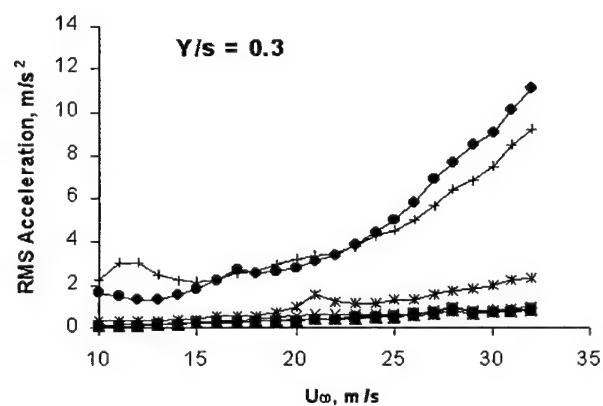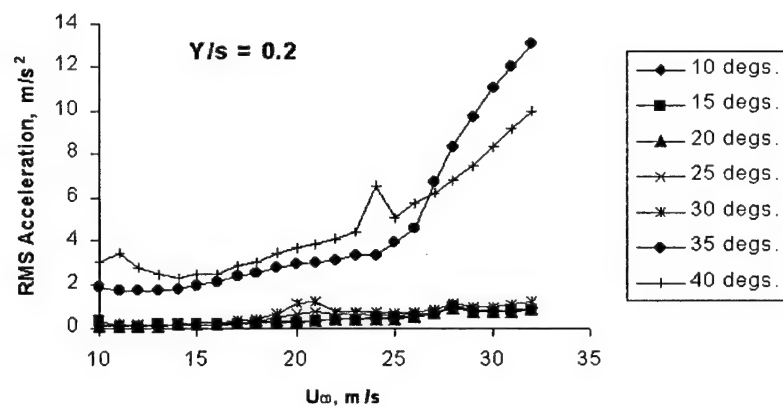
Figure 6
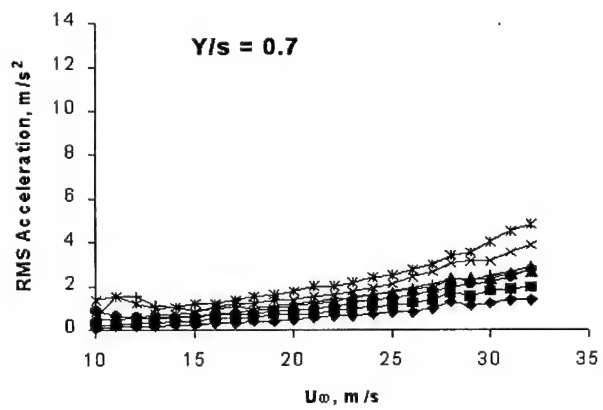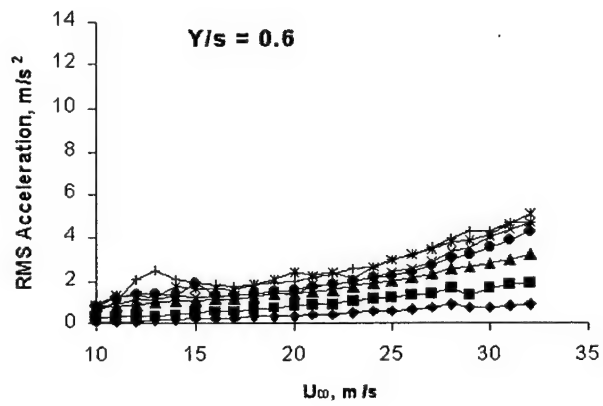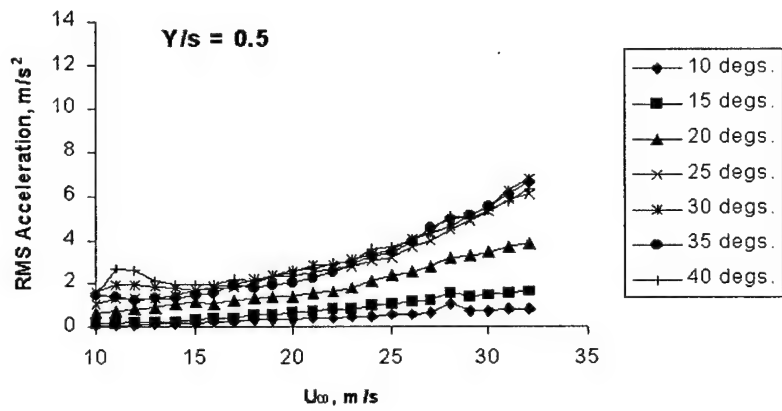
Figure 6
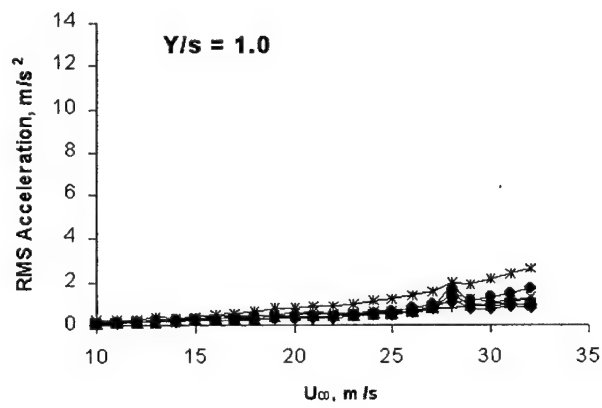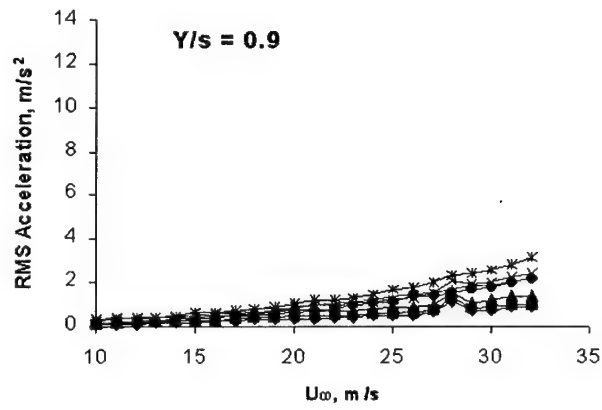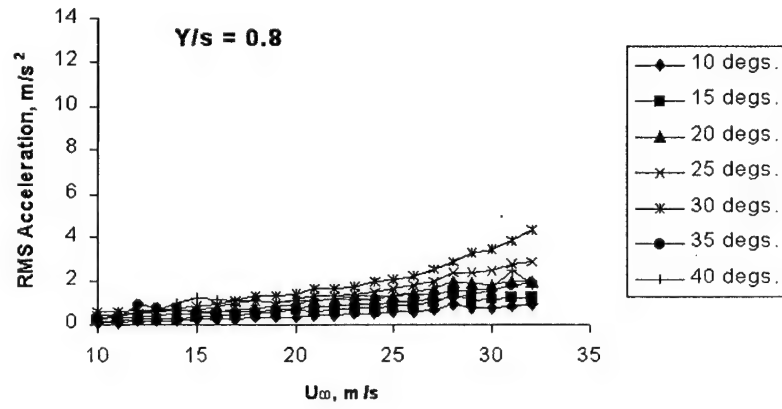
Figure 6: Variation of the root-mean-square value of fin tip acceleration as a function of free stream velocity for different spanwise fin locations.
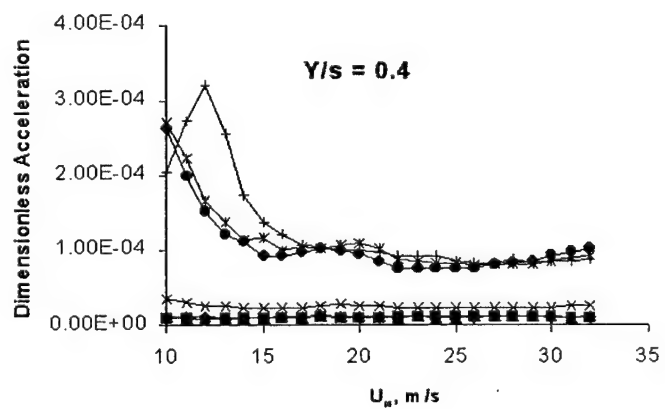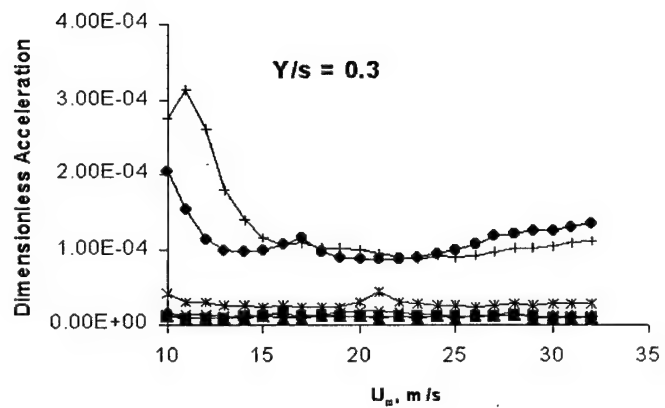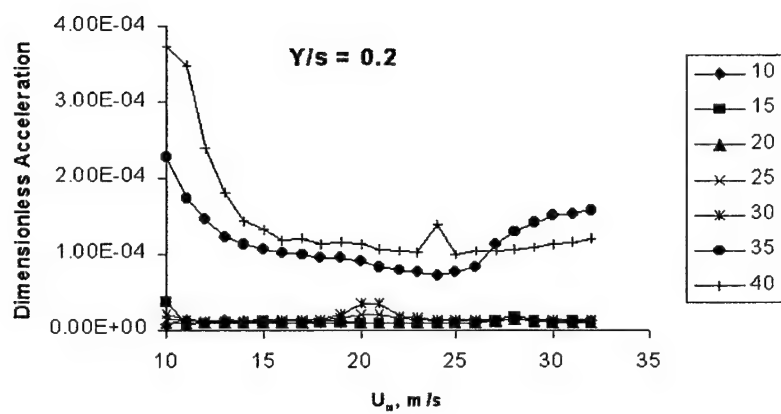
Figure 7
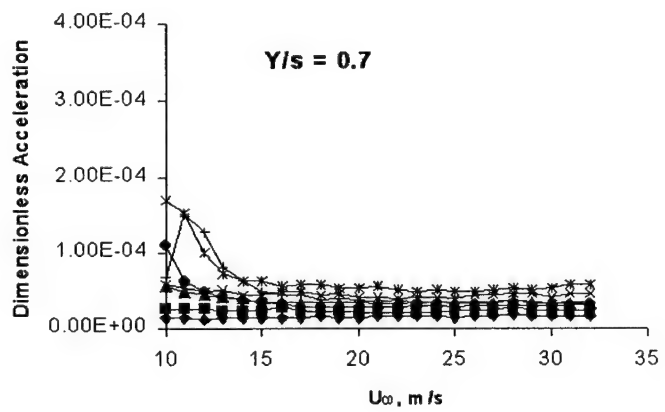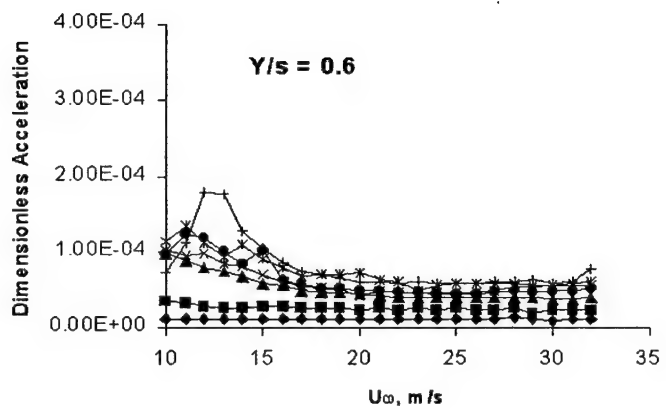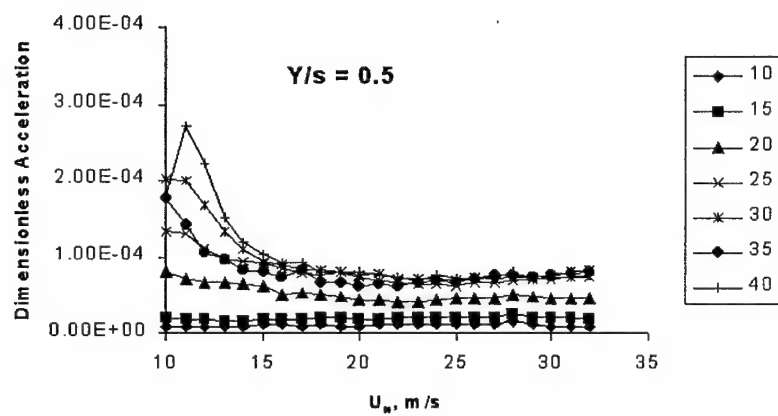
Figure 7
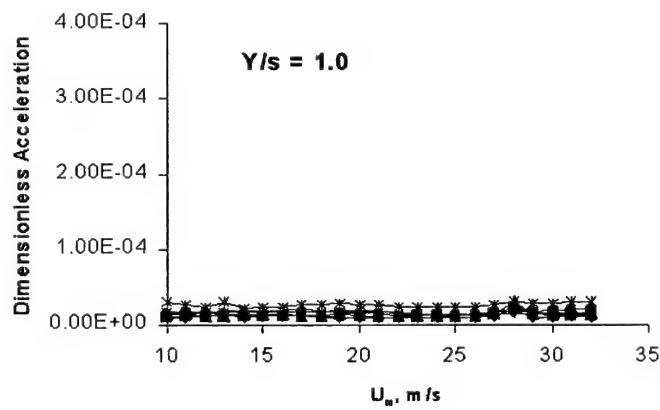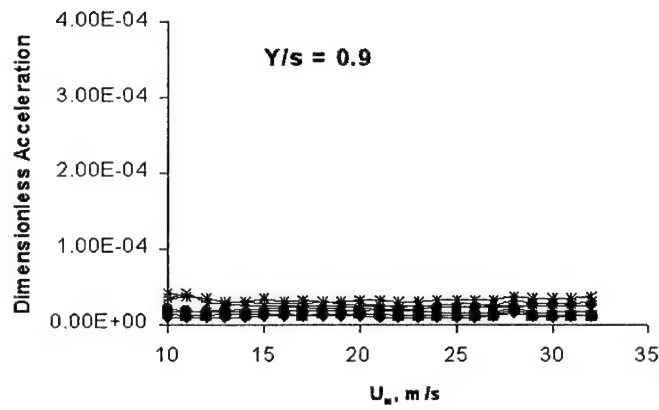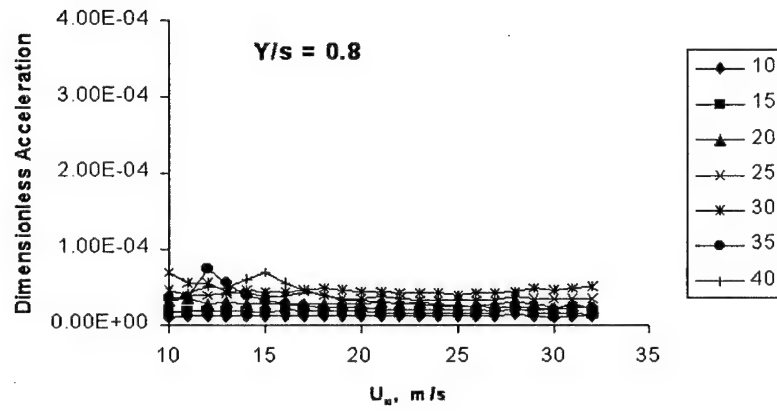
Figure 7: Variation of dimensionless tip acceleration as a function of free stream velocity for different spanwise fin locations.
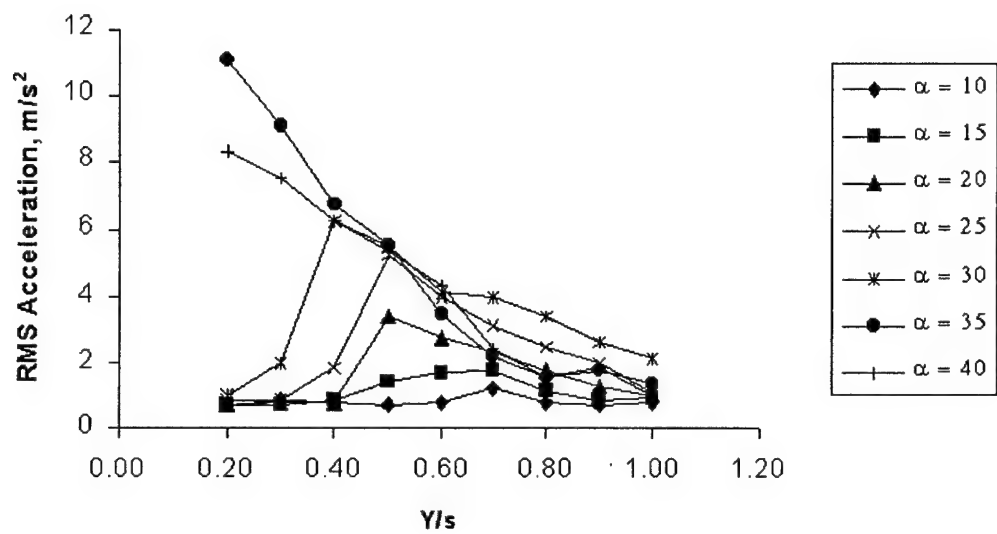
Figure 8: Variation of rms acceleration as a function of fin location for $U_\infty = 30$ m/s.
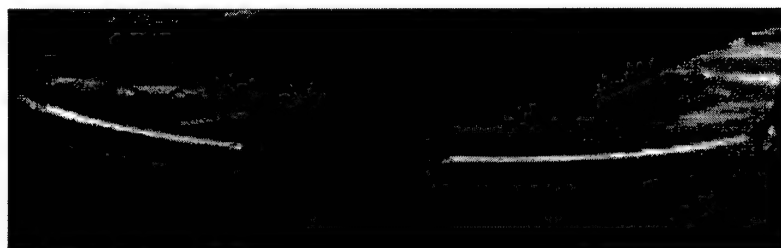
Yf/s = 0.2

Yf/s = 0.4

Yf/s = 0.6

Yf/s = 0.8

Yf/s = 1.0

Figure 9: Flow visualization for different values of fin location for α=30°.
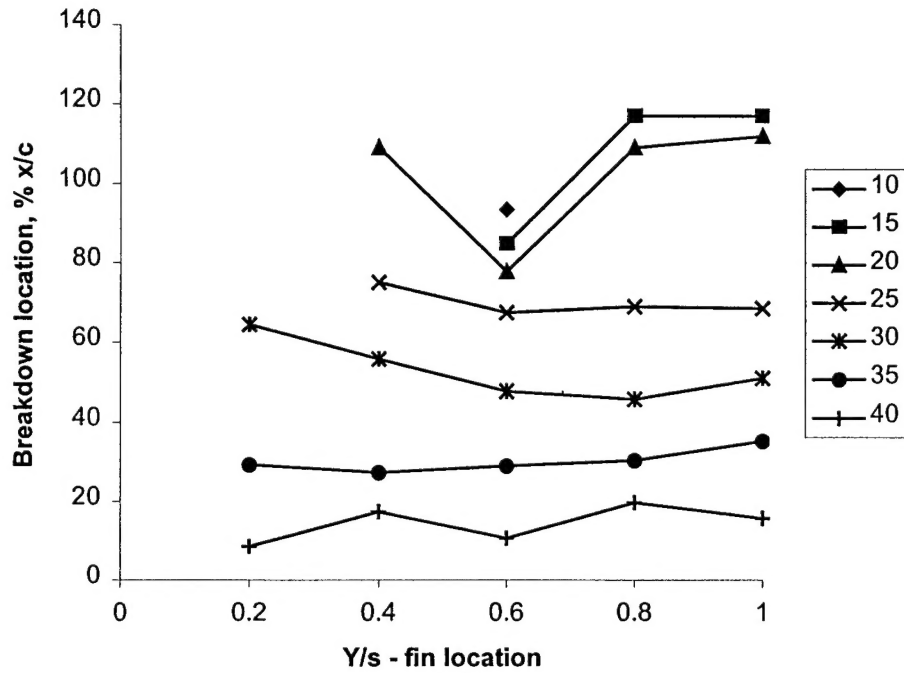
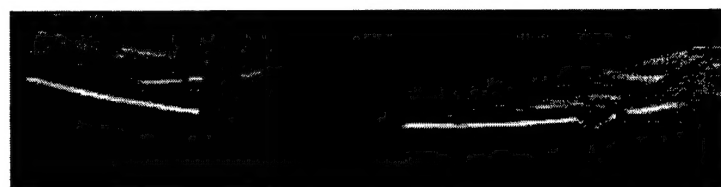Figure 10: Variation of breakdown location as a function of fin location at different angles of attack.
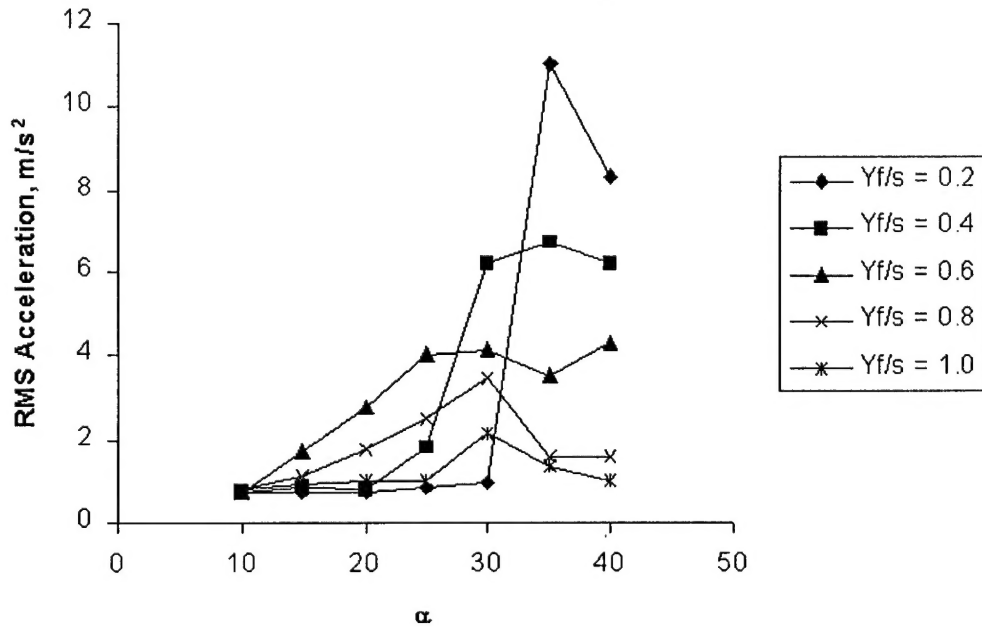
Figure 11: Variation of rms acceleration as a function of angle of attack, $U_\infty = 30$ m/s.
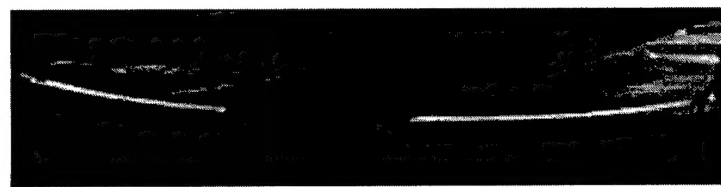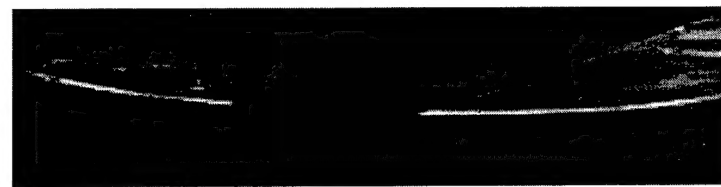
21

$\alpha = 10^{0}$

$\alpha = 15^{0}$

$\alpha = 20^{0}$

$\alpha = 25^{0}$

$\alpha = 30^{0}$

$\alpha = 35^{0}$

$\alpha = 40^{0}$

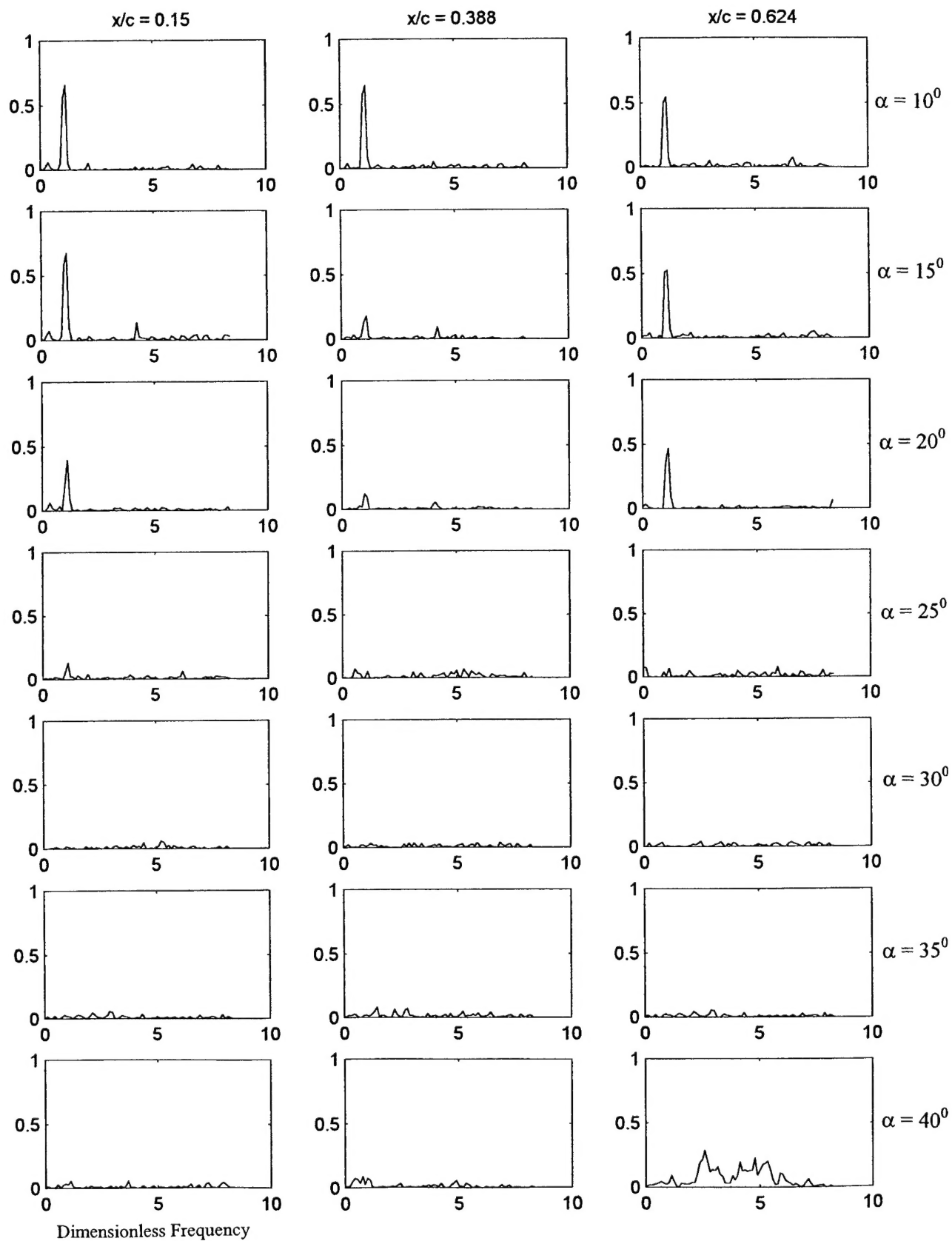Figure 12: Flow visualization for different values of angle of attack for $y_f/s=0.2$.
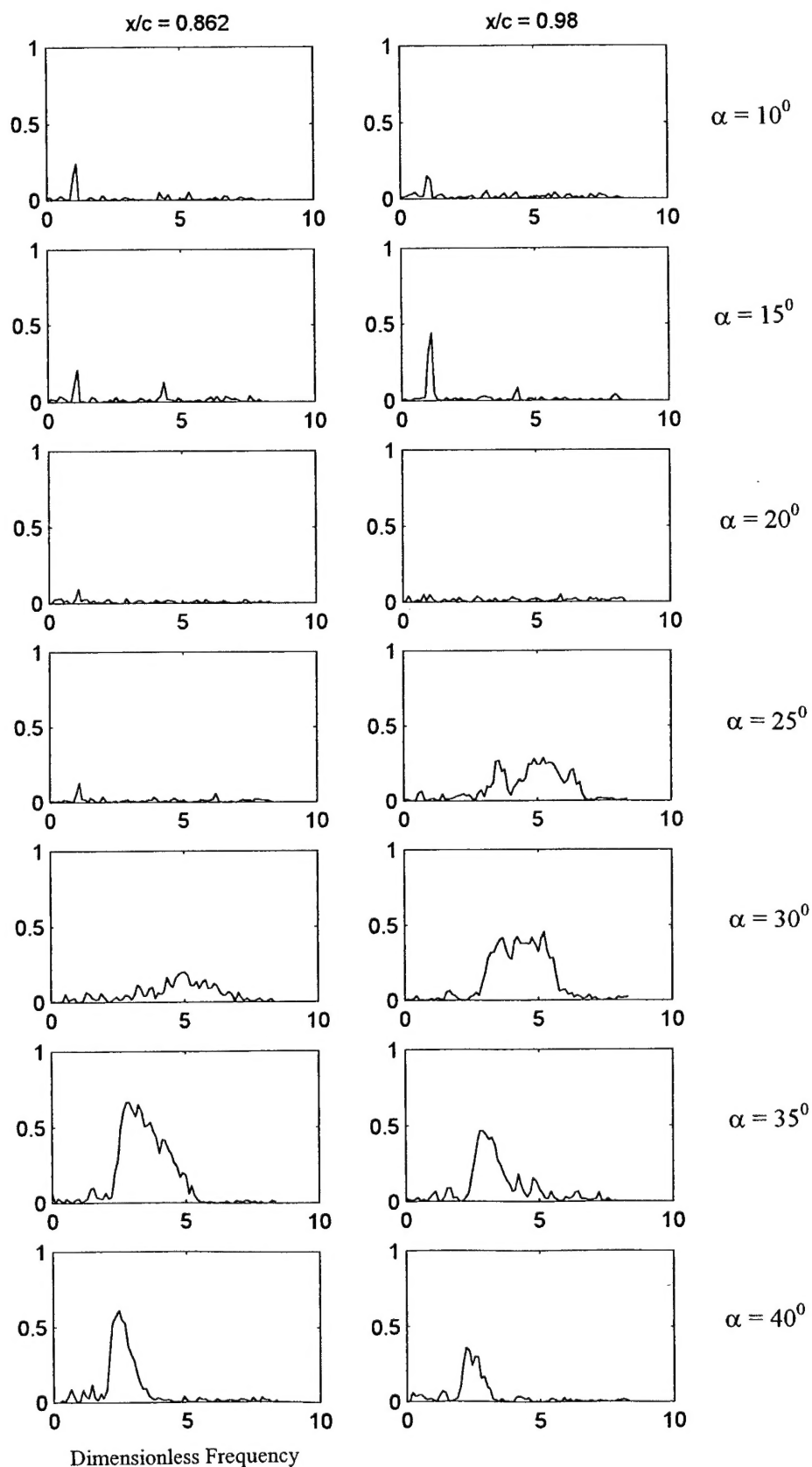
Figure 13

Figure 13: Variation of coherence function between the wing pressure and fin acceleration for different values of angle of attack and streamwise position of pressure transducer.